Physicochem. Probl. Miner. Process., 58(6), 2022, 156349

http://www.journalssystem.com/ppmp

Physicochemical Problems of Mineral Processing

ISSN 1643-1049

Mechanistic study on the flotation of barite with $C_{18}H_{33}NaO_2$ under microwave radiation based on UV-visible spectrophotometric analysis

Jing Guo [1,2,3], Ming Wen [2], Jingxuan Wu [2]

[1] China University of Mining and Technology (Beijing), China

[2] Key Laboratory of Integrated Exploitation of Bayan Obo Multi-Metal Resources, Inner Mongolia University of Science and Technology, Baotou 014010, China

[3] Jin Neng Holding Coal Group, Datong 037300, China

Corresponding author: yizeown@163.com (Jing Guo)

Abstract: Based on the pure mineral flotation tests of barite, this study investigated the effect law of microwave on barite flotation by using a UV-visible spectrophotometer (L5), solution chemistry calculation, and zeta potential, scanning electron microscope (SEM), and other testing methods. Additionally, red flotation kinetic analysis was carried out to deeply explore the mechanism of $C_{18}H_{33}NaO_2$ flotation of barite under microwave radiation. Mineral flotation tests showed that after microwave treatment, the flotation recovery of barite and deionized water increased by 2.67% and 3.35%, respectively, while that of the microwave action pulp and chemically added pulp decreased by 2.90% and 8.51%, respectively. Microwave action on barite can improve its flotation recovery (up to 95.27%). The action of microwave heating can improve the positive electrical properties of the surface of barite, and accordingly, its specific surface area would be enlarged. In this case, the adsorption rate of sodium oleate on the surface of barite increased, thereby improving the flotation recovery. The flotation kinetics analysis revealed that the k-value of the primary kinetic model was the most informative among the four models of flotation kinetics, and its fitting results can truly reflect the flotation results of barite before and after the microwave action. Through the analysis of barite flotation adsorption experiment under microwave action and with sodium oleate as a collector, this study revealed the mechanism of $C_{18}H_{33}NaO_2$ on barite flotation under a microwave roaster. This study provides an important reference for the research on efficient barite flotation.

Keywords: UV-visible spectrophotometer, microwave, barite, flotation mechanism

1. Introduction

Barite is the most common mineral of barium salt, whose main component is barium sulfate ($BaSO_4$). It is chemically stable, insoluble in water and hydrochloric acid, non-magnetic and toxic, and can absorb α-rays, β-rays and γ-rays and other characteristics (Ogwuegbu et al., 2011; Haruo and Yoshio, 2014; Nuria et al., 2015; Kasia et al., 2016; Lu et al., 2020). Due to the chemical stability of barite, solid barium compounds made from barite are widely used in the fields of new energy (Zhao et al., 2014; Zhou et al., 2020; Cen et al., 2021; Liu et al., 2021), new materials, chemical industry, petroleum, light industry, atomic energy, military, building materials, medicine, agriculture, plastics, paper making, capacitors, semiconductors, electronic ceramics and other fields and industries (Gurpinar et al., 2004; Cristina et al. 2015; Xiong et al. 2020; Sadik, 2017; Obaidi et al., 2020). In recent years, as the use of barite gradually increases and the recoverable reserves of high-grade barite ore decrease year by year, barite scarcity may occur in the middle and late 21st century. Since the flotation can deal with fine particle size, size and density of the role of small materials, the production process of flotation is mostly used in the sorting and purification process of barite for its treatment (Nantawat and Lek., 2016; Deng et al., 2019; Michele, 2020; Duan et al., 2021; Wang et al., 2021; Wu et al., 2021).

With the continuous progress and development of science and technology, microwave technology, due to its low pollution and high efficiency, is widely used in the pretreatment of minerals to improve

DOI: 10.37190/ppmp/156349

the flotation effect of the agent on the minerals (Fan et al., 2000; Safak et al., 2020. Of the studies on the flotation adsorption of barite ores, Yu (2015) explored the microwave action on deionized water, slurry, and trapping agent on the flotation of fluorite, and found that microwave could improve the flotation recovery of the agent to the mineral. In the whole flotation process, with the addition of an aerophilic hydrophobic trapping agent, the trapping agent molecules on the surface of the minerals would form physical adsorption, chemical adsorption, or physical-chemical adsorption in the flotation tank. In this process, the rising bubbles drive the target minerals up to the top of the tank to achieve the purpose of sorting (Chau et al. 2009; Saththasivam et al., 2016). Wang (2019) used $C_{18}H_{33}NaO_2$, sodium dodecyl sulfate ($C_{12}H_{25}SO_4Na$), octadecylamine ($C_{18}H_{39}N$), hydroxamic acid ($C_{17}H_7NO_3$), and soap ($C_{17}H_{35}COONa$) as trapping agents for flotation experiments of barite ore, and found that $C_{18}H_{33}NaO_2$ had the best flotation effect on barite. Sodium oleate would induce chemical adsorption on the surface of barite (Wu et al. 2021). In the process of flotation test research, a series of studies have been conducted mainly in terms of flotation recovery and instrumental characterization (Jiang et al. 2020). However, there are few studies on the use of microwave technology for barite in the $C_{18}H_{33}NaO_2$ flotation process. Accordingly, it is of great necessity to explore the microwave flotation mechanism and investigate the relationship between adsorption and flotation recovery. To be specific, the issues to be addressed include but are not limited to why $C_{18}H_{33}NaO_2$ would be adsorbed on the surface of the mineral, what kind of adsorption it is, and how much agent it needs to achieve maximum effect.

In this study, the adsorption amount of the agent on the surface of barite ore under different conditions was calculated by a UV-visible spectrophotometer (Brijlesh et al., 2018). Through the changes in the specific surface area of minerals before and after the microwave action, the influence law of microwave on barite flotation was revealed. Meanwhile, the colloidal stability and species distribution of sodium oleate in an aqueous solution were determined in combination with the solution adsorption method to explore the adsorption mechanism of microwave action on sodium oleate flotation of barite. This study provides theoretical guidance for the production process of microwave heating technology for barite flotation.

2. Materials and methods

2.1. Experimental materials and equipment

The barite ($BaSO_4$) sample used in this study was obtained from a mine in Henan Province, China, with a particle size of 0.1~0.5 cm. The results of XRF (Shimadzu LABCENTERXRF-1800 fluorescence spectrometer, Japan) physical phase analysis are shown in Table 1, with the $BaSO_4$ content being about 90.8067%. As there are visible black particles in the original barite ore, they were removed by hand sorting, and then the experimental barite was crushed and ground by XRF (X-ray Fluorescence Spectrometry). The results of the XRF physical phase analysis are shown in Table 2, and the $BaSO_4$ content is about 95.6498%. The black particles are potassium feldspar.

Experimental trapping agent $C_{18}H_{33}NaO_2$ (NaOl) and pH adjustment reagent (NaOH, HCl) were analytically pure, and the experimental water was deionized (DI) water with a resistivity of 18.25 MΩ-cm. Equipment: XFGCII-35 inflatable hanging tank flotation machine (Jilin Exploration Machinery

Table 1. XRF analysis results of raw barite ore (%)

BaO	SO_3	CO_2	SiO_2	CaO	Na_2O	Fe_2O_3	MnO	NiO	MgO	K_2O	Al_2O_3
58.87	31.93	3.84	2.89	1.57	0.37	0.10	0.02	0.01	0.08	0.03	0.28

Table 2. XRF analysis results of hand-selected barite (%)

BaO	SO_3	SiO_2	CaO	Na_2O	Fe_2O_3	MnO	MgO	MnO
62.53	33.13	2.35	1.21	0.36	0.10	0.08	0.08	0.02

Table 3. XRF analysis results of experimental barite ore (%)

BaO	SO_3	SiO_2	CaO	Na2O	Fe2O3	Al_2O3
63.20	32.99	2.44	0.73	0.34	0.23	0.07

Factory); Galanz (G80W23CSP-Z) microwave oven (output power: 800W, rated microwave frequency: 2450MHz).

2.2. Experimental process

As shown in Fig. 1, the barite is insoluble in HCl acid. Firstly, the barite ore was placed in 1% HCl acid solution after hand-selection; then the surface oxides were removed by ultrasonication for 15 min, and then the barite ore was dried naturally. In this way, the experimental ore was obtained after crushing and grinding. The experimental ore with a grade of ≥95% was selected for the general flotation mineral mechanism study to meet the experimental requirements. The sonicated barite ore was manually crushed to about 0.01~0.1 cm and ground by a three-head mill to -0.074 mm accounting for 97% of the experimental ore, in preparation for subsequent flotation adsorption experiments as well as mechanistic studies.

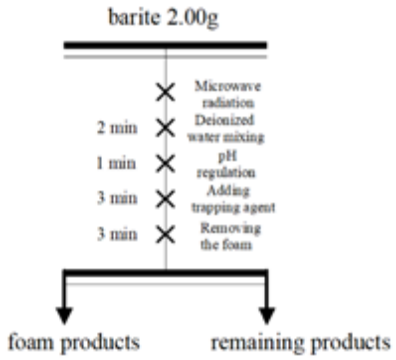

Fig. 2. Schematic diagram of the experimental process

The SEM images of the barite particles at different magnifications are shown in Fig 2, from which it can be seen that the barite particles are irregular in shape and show a laminar structure with tiny barite particles attached to the surface.

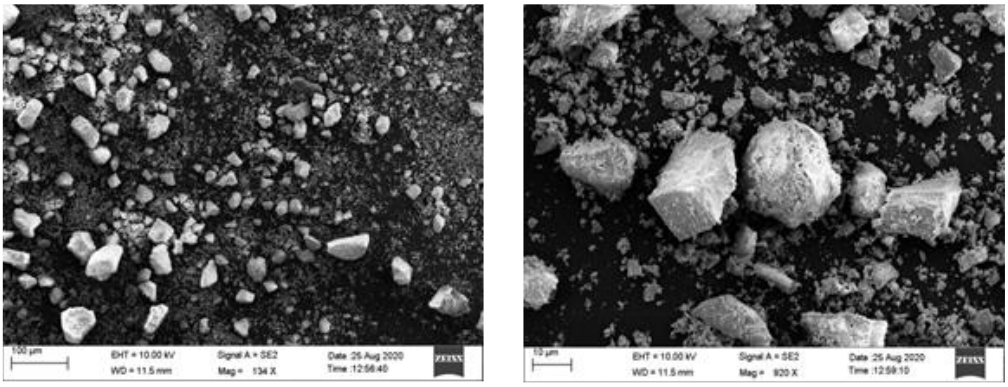

Fig. 1. Electron micrographs of barite particles under different magnifications

2.3. Analytical process

The absorbance of $C_{18}H_{33}NaO_2$ at different dosages was measured by an L5S UV-vis spectrophotometer (Shanghai Electric Analysis Instrument Co., LTD.), and the relationship curve between $C_{18}H_{33}NaO_2$ dosage and absorbance was drawn. At room temperature (22±3°C), 2.0000(±0.0003) g of ore and deionized water were added to the flotation tank with a volume of 30 cm^3 and stirred for 2 min; the slurry was adjusted for 1 min, and the flotation tank was stirred for 3min and then left for 5 min; and 8 cm^3 of the supernatant was pipetted into a centrifuge tube (the volume of the tube was 10 cm^3) and put into a centrifuge for centrifugation (10000 rpm×15 min). After centrifugation, 3 cm^3 of supernatant was pipetted into a quartz cuvette with a pipette gun. The absorbance was measured by a UV-visible spectrophotometer, and then the change of specific surface area was calculated by the solution

adsorption method. By comparing the absorbance of the $C_{18}H_{33}NaO_2$ concentration relationship curve, the corresponding residual could be revealed. The adsorption rate R_1 could be calculated by Eq. 1:

$$R_1 = \frac{C_0 - C_1}{C_0} \times 100\% \quad (1)$$

where: C_0 denotes the initial concentration of $C_{18}H_{33}NaO_2$ added in the flotation experiment (mg/dm³); C_1 refers to the residual concentration of $C_{18}H_{33}NaO_2$ obtained after flotation experiments (mg/dm³).

The absorbance of different $C_{18}H_{33}NaO_2$ dosages was measured by the UV-visible spectrophotometer at the concentrations of 20, 40, 50, 60, 80, and 100 mg/dm³. The absorbance curve of $C_{18}H_{33}NaO_2$ as a function of dosage ($Y = 0.0065X$ ($R^2 = 0.995$)) was plotted and shown in Fig 3.

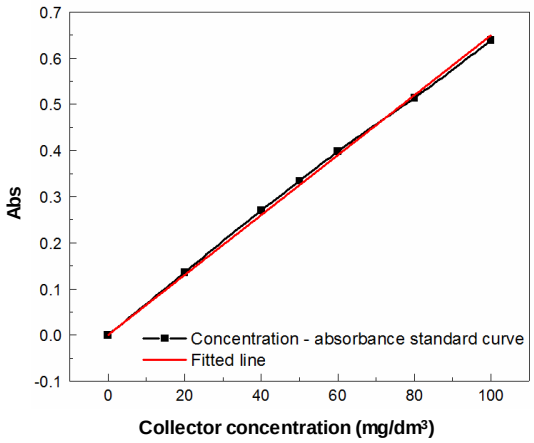

Fig 3. $C_{18}H_{33}NaO_2$ dosage -absorbance relationship graph

3. Results and discussion

3.1. Microwave Radiation Adsorption Parameter

3.1.1. Effect of different sodium oleate dosages and pH values on the flotation of barite

Fig. 4(a) shows the adsorption diagram of barite flotation at different trap concentrations. When the pH is 7, the adsorption rate of sodium oleate on barite ore increases with the increase of sodium oleate dosage. The adsorption rate of sodium oleate on barite ore is 80.85% when the dosage of sodium oleate is 55 mg/dm³, and the adsorption rate of sodium oleate on barite ore increases slightly when the dosage of sodium oleate exceeds 55 mg/dm³. The highest adsorption rate of sodium oleate on barite ore reaches 83.08% when the amount of sodium oleate is 80 mg/dm³. It can be assumed that the adsorption rate of sodium oleate on barite ore is 83.08% when the amount of sodium oleate is 55 mg/dm³, and sodium oleate is chemisorbed with barite ore. After the dosage exceeds 55 mg/dm³, sodium oleate forms physical adsorption on the outer layer of barite. When the sodium oleate dosage is greater than 80 mg/dm³, the adsorption rate of sodium oleate on barite decreases slightly and then remains stable.

Fig. 4(b) shows the effect of different pH values on the adsorption of barite flotation. According to Fig. 4(a), when the amount of sodium oleate is 55 mg/dm³, the adsorption rate of sodium oleate on barite ore increases with the rise of pH value, and the recovery rate gradually stabilizes above 90% when the pH value ranges from 7 to 9, which coincides with the species distribution of sodium oleate in the aqueous solution. The adsorption rate of sodium oleate on barite ore increases slightly; and when the amount of sodium oleate gradually increases, the highest adsorption rate reaches 82.51% at pH 8. Combined with the analysis of flotation experiments, it can be seen that the optimum pH value for flotation of barite is between 7 and 9, which is consistent with the chemical calculation settlement of sodium oleate flotation solution.

3.1.2. Microwave flotation experiment

As seen from Fig. 5(a), the results of the flotation and adsorption experiments on barite after 30 sec of microwave action at pH 7 were compared with the flotation and adsorption experiments before the microwave action. The adsorption rate after 30 sec of microwave action on barite increases up to 85.29%

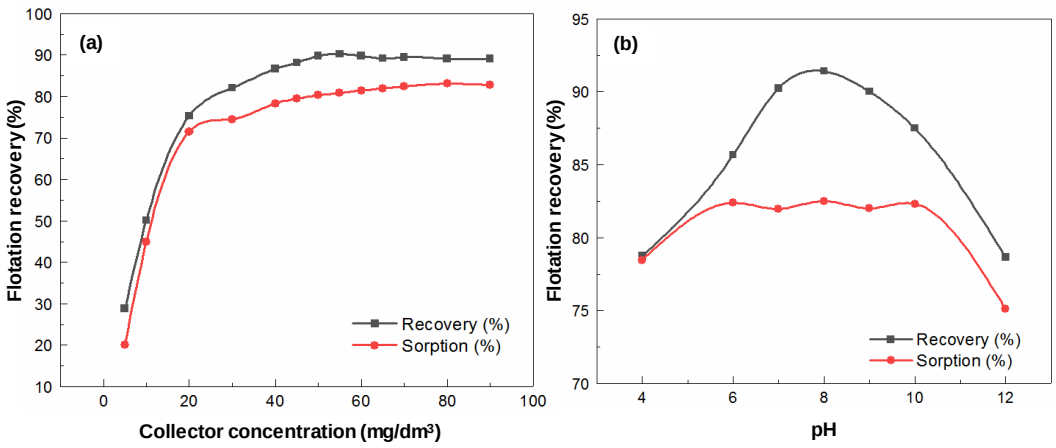

Fig 4. Effect of different parameters on the adsorption rate of flotation barite (a: trap concentration; b: pH)

when the dosage of sodium oleate is 55 mg/dm^3, an increase of 4.44%. When the amount of sodium oleate exceeds 70 mg/dm^3, the adsorption rate after 30 sec of microwave action on barite slightly decreases and then stabilizes.

Fig. 5(b) shows the comparison of the flotation and adsorption experiments of DI water before and after 30 sec of microwave action at pH 7. After 30 sec of microwave action, the adsorption rate of DI water increases up to 84.84% at the dosage of 55 mg/dm^3 of sodium oleate, an increase of 3.99%. The highest adsorption rate is 83.42% after 30 sec of microwave action. When the amount of sodium oleate exceeds 65 mg/dm^3, the adsorption rate of DI water decreased slightly decreases and then becomes stable. Comparing Fig. 5(a) and Fig. 5(b), it is found that the flotation recovery after 30 sec of microwave action on barite is 1.53% lower; and the adsorption rate is 0.45% higher than that after 30 sec of microwave action on DI water at a dosage of 55 mg/dm^3 of sodium oleate and pH 7. This indicates that the microwave action on barite may cause stress and thermal expansion at the mineral particle interface and increase the specific surface area, thus making sodium oleate better for adsorption with barite and improving the adsorption rate of minerals. The adsorption rate of sodium oleate to minerals is improved by the adsorption of sodium oleate to barite. It can be deduced that microwave action has a great effect on water in terms of absorption. Through microwave treatment, the water temperature can increase quickly, thus increasing the activity of water molecules. Consequently, sodium oleate in water could be dissolved more quickly and distributed uniformly in the solution. In this sense, sodium oleate has a trapping effect on the barite ore, thus improving the flotation effect.

As shown in Fig. 5 (c), when pH is 7, flotation and adsorption experiments are conducted on the pulp after 30 sec of microwave action. The results are compared with those of the flotation and adsorption experiments before the microwave action. When the amount of sodium oleate is greater than 55 mg/dm^3, the recovery rate after 30 sec of microwave action gradually decreases and stabilizes at 80 mg·L^{-1}, and the flotation recovery rate is about 79%; the adsorption rate after 30 sec of microwave action also decreases at 55 mg/dm^3. When the amount of sodium oleate exceeds 70 mg/dm^3, the adsorption rate of microwave-operated pulp after 30 seconds of microwave action decreases slightly and becomes stable. Comparing Fig. 5(a), Fig. 5(b), and Fig. 5(c), it could be found that: at the dosage of 55 mg/dm^3 of sodium oleate, the flotation recovery, and adsorption rate decreases after 30 sec of microwave action on the pulp, indicating that the microwave action on the pulp can increase the activity of water molecules in the DI water and the temperature of the pulp, thus increasing the dissolution of some barite in the DI water and achieving a better effect. After adding the trapping agent, the trapping group cannot fully combine with the barite, thus reducing the adsorption effect. The addition of the trapping agent will reduce the adsorption effect and lower the flotation recovery.

Fig. 5(d) shows the effects of microwave barite, DI water, slurry, and slurry after adding a trapping agent for 5, 10, 30, 60, and 90 sec, respectively, on the recovery rate of sodium oleate. As can be seen from Fig. 5(d), the flotation recovery effect of microwave barite and DI water is the best within 5-30 sec; the recovery rate tends to be stable within 30-90 sec of microwave action; and when the microwave time exceeds 90 sec, the recovery rate decreases. The recovery rate experiences the sharpest decline when the

microwave slurry time is within 5-30 sec. When the microwave time is more than 30 sec, the flotation recovery tends to stabilize within a certain range; and with the increase in time, the effect does not display any obvious change. Mineral flotation tests show that with microwave treatment, the flotation recovery rate of barite and DI water increases by 2.67% and 3.35%, while that of the microwave action pulp and chemically added pulp decreases by 2.90% and 8.51%, respectively. Microwave action barite can improve flotation recovery (up to 95.27%).

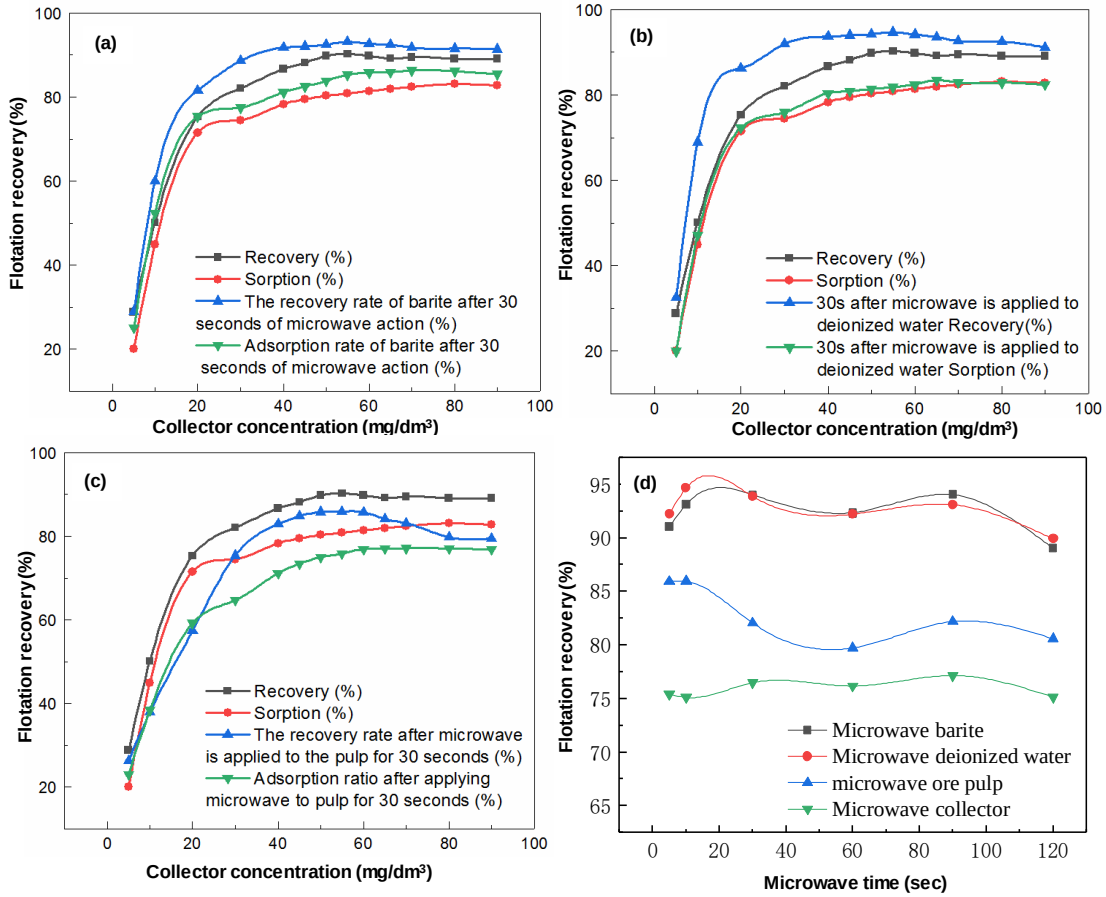

Fig. 5. Effect of trapping agent on barite flotation under different conditions of microwave radiation (a: adsorption relationship of flotation before and after microwave radiation on barite at different trap concentrations; b: adsorption diagram of flotation before and after microwave action on DI water with different trap concentrations; c: adsorption diagram of flotation before and after microwave radiation pulp with different trap concentrations; d: effect of different microwave radiation time on the recovery rate)

3.2. Adsorption mechanism of microwave radiation

3.2.1. Solution chemistry calculations

In this study, sodium oleate ($C_{18}H_{33}NaO_2$) was chosen as the flotation agent at room temperature during flotation, and its corresponding solubility is $10^{-7.6}$ mol/dm³. By reviewing the relevant literature, it can be known that the main hydrolysis reaction occurs in water, and the dissolved and undissolved agents reach a stable equilibrium state, with four main equilibrium relationships, as shown in Table 4.

Table 4. Equilibrium relationships of dissolution reaction of $C_{18}H_{33}NaO_2$ in aqueous solution

Balance relationship	Balance equation	lgK
Dissolution equilibrium	$HOl_{(l)} \leftrightharpoons HOl_{(aq)}$	-7.6
Dissociation equilibrium	$HOl_{(aq)} \leftrightharpoons H^+ + Ol^-$	-4.95
Trimeric balance	$2Ol^- \leftrightharpoons (Ol^-)_2^{2-}$	4.0
Acid soap dimerization balance	$HOl_{(aq)} + Ol^- \leftrightharpoons H(Ol)^{2-}$	4.7

The agent is present in an aqueous solution as five components: liquid $C_{18}H_{33}NaO_2$, solid $C_{18}H_{33}NaO_2$, $RCOOH^-$ (monomer), $(RCOOH)^{2-}$ (dimer), and RCOOH-RCOOH- (molecular-ionic conjugate). The logarithmic plot of the concentration of each component, C, with pH is shown in Fig. 6.

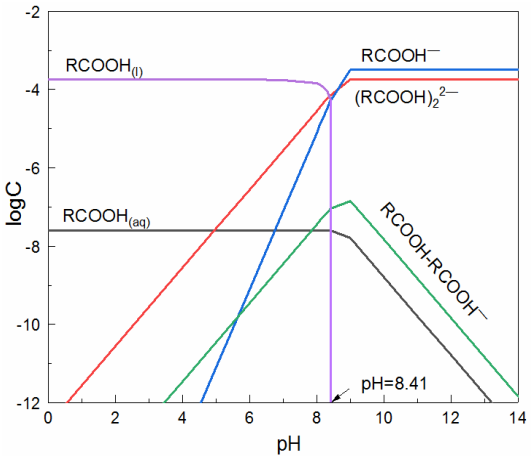

Fig. 6. Chemical calculation of $C_{18}H_{33}NaO_2$ solution

The critical pH value of $C_{18}H_{33}NaO_2$ at a concentration of 55 mg/dm^3 is 8.41. Under strong acid conditions, the solution is mainly present as the $RCOOH_{(l)}$, and $RCOOH_{(aq)}$ fractions; and when the pH value is between 3.5 and 8.41, all five fractions are present, of which the amount of oleic acid molecules is higher relative to the amount of other molecules; and the concentrations of monomers, dimers, and molecular-ionic congeners would increase as the concentration of monomers, dimers, and molecular-ionic conjugates gradually increase which is in turn triggered by the increase of alkalinity in the aqueous solution. When the pH value is between 8.41 and 13, the concentrations of ionic $RCOOH^-$ and $(RCOOH)^{2-}$ components tend to stabilize; the concentrations of $RCOOH_{(aq)}$ and molecular-ionic conjugates RCOOH-$RCOOH^-$ decrease with the rise of pH value, and the $RCOOH_{(l)}$ component is not present. Under strong alkaline conditions, the solution is mainly composed of $RCOOH^-$ and $(RCOOH)^{2-}$ components. In the specific trapping process, because the structure of the conjugate is larger than that of other ions, it can better adsorb with the minerals under the same environment; the adsorption amount increases with the increase of stirring time, which enhances the hydrophobicity of the barite surface, thus obtaining a better trapping effect. Therefore, it can be concluded that the molecular-ionic conjugate RCOOH-$RCOOH^-$ is the main active component of $C_{18}H_{33}NaO_2$ flotation of barite.

3.2.2. Zeta potential analysis

Fig. 7 shows the zeta potential plots at different pH conditions. According to Fig. 7, curve (1) shows the test results of the microwave barite 10 sec; curve (2) displays the test results of the microwave deionized water 10 sec; curve (3) presents the test results of microwave ore pulp 10 sec, and curve (4) shows the test results of barite and DI water without any microwave radiation.

As can be seen from Fig. 7, the isoelectric point of the slurry appears at pH 4.02 or so in Curve (4), at pH 4.58 or so in Curve (1), at pH 4.35 or so in Curve (2), and at pH 5.85 or so in Curve (3). The isoelectric points after the microwave are positively shifted, and the most remarkable shift appears in the microwave ore pulp. Under acidic conditions, with more H^+ than OH^-, barite is insoluble in water at room temperature. The microwave radiation would raise the temperature of the slurry so that part of the barite dissociates due to the surface of the colloidal dispersion particles with a negative charge and attracts the surrounding positively-charged ions. Accordingly, part of the SO_4^{2-} would combine H^+, thereby reducing the H^+ in the colloid and indirectly shielding the surface of the colloid. Therefore, the isoelectric point of the colloidal dispersion system is increased. Microwave radiation before the micellar dispersion system is more stable under alkaline conditions than under acidic conditions, displaying a stronger resistance to aggregation. After the microwave radiation, the stability of barite and deionized water, in acidic and alkaline conditions, remains the same. After the microwave radiation of mineral slurry, the micellar dispersion system is more stable under acidic conditions than under alkaline

conditions, showing a stronger resistance to aggregation and being less inclined to coagulation or coalescence.

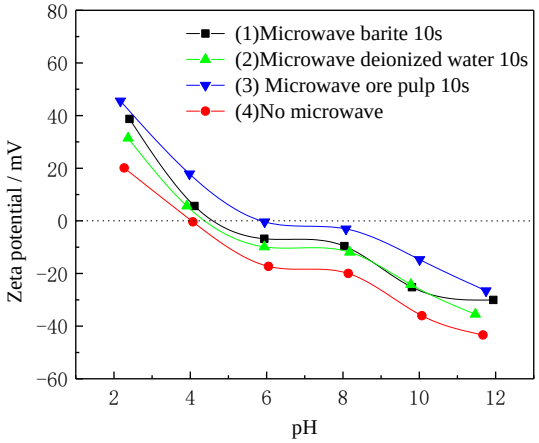

Fig. 7. Zeta potential plots at different pH conditions

3.2.3. Analysis of change in specific surface area

The specific surface area of fatty acids and dyes on mineral surfaces is generally determined by the solution adsorption method, which is mainly due to the formation of hydrogen bonds between the fatty acid molecules and the mineral surfaces in actual solution, or the chemisorption of salts with oxygenated surfaces. The flotation adsorption diagram of the fatty acid trap ($C_{18}H_{33}NaO_2$) and barite ore is shown in Fig. 8.

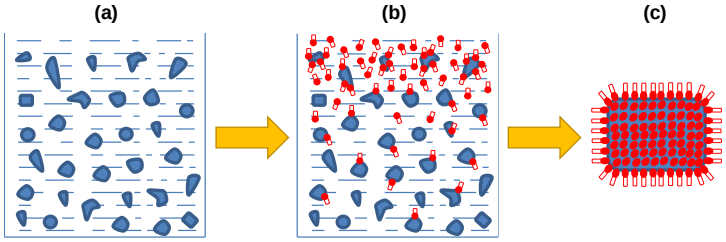

Fig. 8. Adsorption diagram of flotation before and after microwave radiation pulp with different trap concentrations

Fig. 8 (a) shows the uniform distribution of barite ore in an aqueous solution before adding the trap; Fig. 8 (b) shows the distribution state when the trap is just added; Fig. 8 (c) shows that the $C_{18}H_{33}NaO_2$ molecules are more uniform, compact and adsorbed on the surface of barite ore in a single molecular layer after agitation. The adsorption rate of $C_{18}H_{33}NaO_2$ on the surface of barite under different conditions is calculated by a UV-visible spectrophotometer, and then the specific surface area is determined according to the solution adsorption method, etc. In an aqueous solution, the adsorption force of the agent on the mineral surface is calculated as (x/m) m. The cross-sectional area of the agent molecules is S_0, and the specific surface area of S can be calculated according to Eq. 2:

$$S = (x/m)_m \times N_A \times S_0 \tag{2}$$

where $(x/m)_m$ denotes the amount of agent attached to the mineral surface at the time of stabilization under the Langmuir monolayer (mol/g); N_A is the Avogadro constants, (/mol); S_0 is the cross-sectional area of solute molecules (nm²). According to the adsorption amount of the solution Γ:

$$\Gamma = x/m = [(C_0\text{-}C_1)v]/m \tag{3}$$

where v is the solution volume; m denotes the quality of pharmaceuticals. According to the Langmuir formula in solution adsorption:

$$x/m = [(x/m)_m bc_1]/(1 + bc_1) \tag{4}$$

where b is the constant, mainly related to the heat of adsorption.

Combining Eqs. (2), (3), and (4), it can be seen that in the same test environment, the specific surface (area) ratio (S_1/S_2) of any two different microwave radiation times at the same concentration is proportional to its adsorption volume ratio under the same conditions and proportional to the concentration of the adsorbed $C_{18}H_{33}NaO_2$. The solution adsorption method is usually used to calculate the corresponding specific surface area. There are a total of two different types, namely fatty acids and dyes, which are generally adsorbed on the mineral surface as a single molecular layer of molecules. Combined with the determination of specific surface (area) by solution adsorption method, it is known that the specific surface (area) of any two different microwave radiation cases at the same concentration in the same test environment is proportional to its adsorption under the same conditions and proportional to the concentration of $C_{18}H_{33}NaO_2$ adsorbed, which could be expressed as follows:

$$\frac{S_a}{b} = \frac{\Gamma_a}{\Gamma_b} = \frac{c_a}{c_b} \tag{5}$$

Under the condition of microwave radiation of barite for 30 sec, the changes in adsorption concentration of pharmaceuticals before and after microwave radiation of barite are shown in Table 5 and Table 6.

Table 5. Adsorption concentration before microwave radiation

Serial number	$C_{18}H_{33}NaO_2$	Abs	Residual concentration	Adsorption concentration
1	20 mg/dm³	0.0370	5.6923	14.3077
2	40 mg/dm³	0.0564	8.6769	31.3231
3	50 mg/dm³	0.0640	9.8462	40.1538
4	60 mg/dm³	0.0724	11.1385	48.8615
5	80 mg/dm³	0.0880	13.5385	66.4615

Table 6. Adsorption concentration of barite after 30 sec of microwave radiation

Serial number	$C_{18}H_{33}NaO_2$	Abs	Residual concentration	Adsorption
1	20 mg/dm³	0.0320	4.9231	15.0769
2	40 mg/dm³	0.0490	7.5385	32.4615
3	50 mg/dm³	0.0525	8.0772	41.9228
4	60 mg/dm³	0.0552	8.4952	51.5048
5	80 mg/dm³	0.0720	11.0769	68.9231

By comparing the phase results, it can be known that the amount of $C_{18}H_{33}NaO_2$ is 20, 40, 50, 60, and 80 mg/dm³; the specific surface of barite after 30 sec of microwave radiation increases by 5.38%, 3.63%, 4.41%, 5.41%, and 3.70%, respectively, with an average increase of about 4.51%. This indicates that the specific surface (area) of barite ore after 30 s of microwave radiation increases, creates a greater possibility of adsorption between the agent and the mineral, thus changing the flotation effect.

3.2.4. SEM Analysis

The SEM results after the interaction of barite with $C_{18}H_{33}NaO_2$ are shown in Fig. 9. As indicated by the SEM results, there are obvious fine fissures on the surface of barite after the microwave effect. Combined with the results of flotation, adsorption, and specific surface area, it can be concluded that under the same experimental conditions, the flotation, adsorption, and specific surface area of $C_{18}H_{33}NaO_2$ on barite would increase after the microwave effect. With the increase of the specific surface area of barite ore, the adsorption of $C_{18}H_{33}NaO_2$ on the surface of barite can be improved, thus improving the adsorption rate and flotation recovery of $C_{18}H_{33}NaO_2$ on barite ore.

3.3. Analysis of kinetics before and after microwave radiation

3.3.1. Flotation kinetic analysis

For a single mineral, the flotation rate is proportional to the particle concentration in the pulp in the

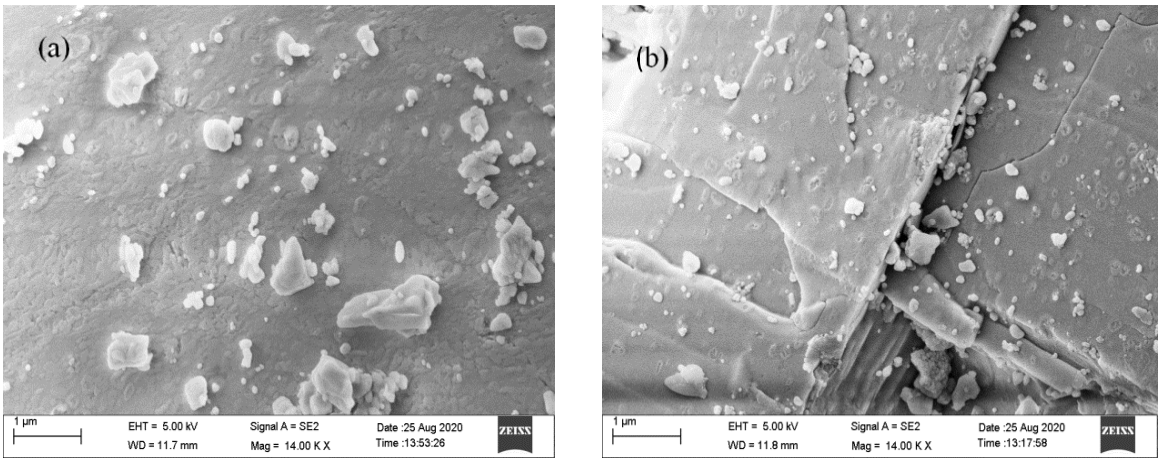

Fig. 9. SEM results after the interaction of barite with $C_{18}H_{33}NaO_2$ under different conditions (a: before microwave radiation; b: after microwave radiation)

flotation cell. The flotation behaviour of barite with $C_{18}H_{33}NaO_2$ as a trapping agent was calculated for the non-microwave radiation (a), microwave radiation on barite (b), microwave radiation on DI water (c), and microwave radiation on slurry (d). The experimental results were fitted using the primary kinetic model (I), primary rectangular distribution model (II), secondary kinetic model (III), and secondary rectangular distribution model (IV) (as presented in Table 7). The flotation recovery versus time under different microwave conditions is shown in Fig. 10. The specific parameters are as follows: $C_{18}H_{33}NaO_2$ dosage: 55 mg/dm^3; pH=7; barite particle size: -200 mesh (75 μm) accounting for 97%; and microwave radiation time: 30 sec.

As is shown in Fig. 10, with the increase of flotation time, the flotation recovery of all microwave radiation conditions increases accordingly; and the flotation recovery of microwave radiation barite and microwave radiation DI is much higher; that of microwave radiation pulp is the lowest. The model fit values at different times were calculated by substituting ε^{∞}=96.18% and the mean value of k-value into

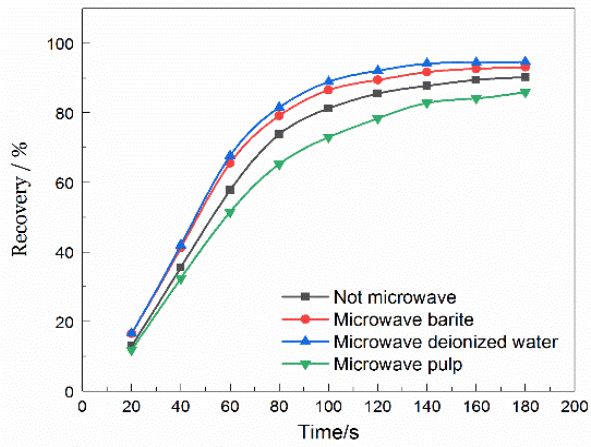

Fig. 10. Relationship between flotation time and recovery under different conditions

Table 7. Flotation kinetic model

NO.	Type	Flotation kinetic model equation Abs
I	Classical Level 1 Model	$\varepsilon = \varepsilon_{\infty}\ (1 - e^{-kt})$
II	One-level rectangular distribution model	$\varepsilon = \varepsilon_{\infty}[1 -\ (1 - e^{-kt})/kt]$
III	Secondary kinetic model	$\varepsilon = \frac{\varepsilon^2{}_{\infty}\ kt}{1 + \varepsilon_{\infty} kt}$
IV	Secondary rectangular distribution model	$\varepsilon = \varepsilon_{\infty}[1 - ln\ (1 + \varepsilon_{\infty} kt)/kt]$

the primary kinetic model (I), primary rectangular distribution model (II), secondary kinetic model (III), and secondary rectangular distribution model (IV), respectively. The time-recovery graphs of the first-level kinetic model (I), the first-level rectangular distribution model (II), the second-level kinetic model (III), and the second-level moment distribution model (IV) are shown in Fig. 11. When the flotation time is within 180s, and the upper limit of the fit is the barite grade value, the first-level kinetic model is the most informative. The k value is the most informative and the fitted results best reflect the real flotation

Table 8. Flotation kinetic model fitting parameters

Condition	Time (sec)	ε (%)	k_{I}	k_{II}	k_{III}	k_{IV}
a	60	57.71	0.01527	0.03724	0.02599	0.06487
	120	85.51	0.01832	0.07510	0.06944	0.25718
	180	90.23	0.01546	0.08982	0.08759	0.37649
b	60	65.54	0.01906	0.04966	0.03707	0.10011
	120	89.47	0.02219	0.11940	0.11550	0.48221
	180	93.12	0.01915	0.17460	0.17590	0.87851
c	60	67.62	0.02024	0.05392	0.04103	0.11344
	120	92.11	0.02635	0.19690	0.19610	0.92071
	180	94.65	0.02300	0.34920	0.35730	2.05199
d	60	51.48	0.01277	0.02990	0.01996	0.04708
	120	78.41	0.01407	0.04490	0.03823	0.12259
	180	85.94	0.01244	0.05209	0.04848	0.18154

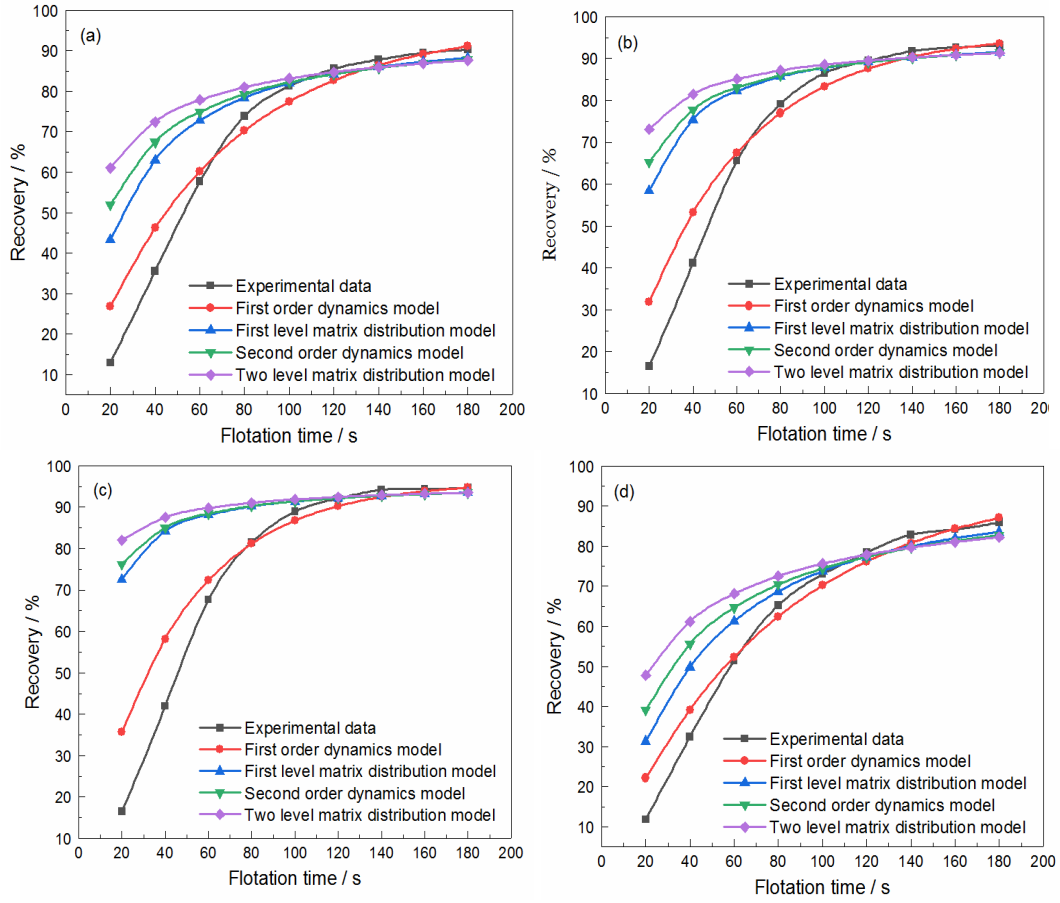

Fig. 11. Comparative analysis of model fit and experimental values under different microwave conditions (a) before microwave radiation (b) microwave radiation barite (c) microwave radiation DI water (d) microwave radiation mineral slurry

results. The kinetic model is compared with those of microwave-activated barite ore, microwave-activated DI water, and microwave-activated slurry, and The first-level kinetic model also has the best reference value when compared with the results of the microwave-activated barite ore, microwave-activated deionized water, microwave-activated slurry, and non-microwave-activated slurry. When the flotation time is less than 70 sec, the results of the first-level kinetic model are higher than the actual values; when the flotation time is longer than 70 sec, the results of the first-order kinetic model are slightly lower than the actual values. When the flotation time is less than 100 sec, the fitted results of the primary rectangular distribution model, secondary kinetic model, and secondary rectangular distribution model are much higher than the actual values. When the flotation time is greater than 100 sec, the results are similar to the actual values.

3.3.2. Adsorption kinetic analysis

The mechanism of sodium oleate adsorption on the surface of barite ore generally includes two types of adsorption: physical adsorption and chemical adsorption. It can be investigated by using UV-visible spectroscopy and adsorption kinetic model calculation to discuss the trapping mode of sodium oleate in barite ore flotation and the relationship with the adsorption behaviour of flotation.

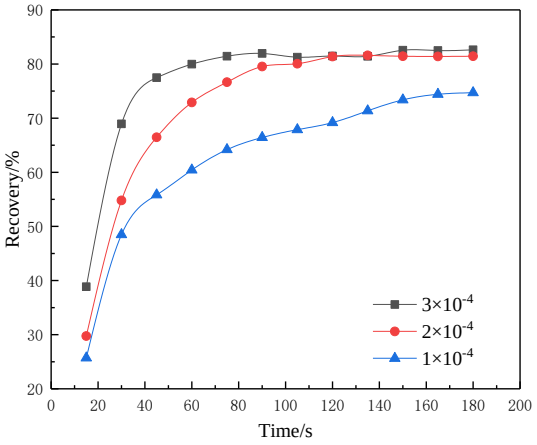

Fig. 12. Adsorption rates of different sodium oleate concentrations on barite at different times

The adsorption kinetic model can be used to study the degree of fast and slow adsorption under different conditions in the flotation adsorption process. On this basis, the adsorption rate constants are calculated by combining the relevant kinetic equations (shown in Table 9) at the concentrations of 1.10^{-4}, 2.10^{-4}, and 3.10^{-4} mol/dm^3 of sodium oleate, respectively. The adsorption behaviour under different conditions is analyzed by the changes in the adsorption rate constants, as shown in Fig. 12. As can be seen from the Fig., the amount of sodium oleate adsorbed by barite increases with time and reaches adsorption equilibrium after a certain time; and the specific adsorption amount at a certain point can be known by the adsorption rate, so that the adsorption kinetics calculation can be performed. The adsorption behaviour of barite with sodium oleate as a trapping agent is investigated by calculating the primary adsorption model, secondary adsorption model, and internal diffusion adsorption model, as well as the fitting analysis of the experimental results. The rate constants corresponding to the three models are calculated and shown in Table 10.

Table 9. Adsorption kinetic model

NO.	Type	Flotation kinetic model equation Abs
I	First stage adsorption kinetic model	$log\ (R_e - R_t) = lnR_e - \frac{K_1}{2.303}t$
II	Second stage adsorption kinetic model	$\frac{t}{R_t} = \frac{1}{h} + \frac{t}{R_e}$
III	Internal diffusion model	$R_t = K_3 t^{1/2}$

Table 10. Relationship between adsorption time and recovery rate at different sodium oleate concentrations

Time/s	First-stage adsorption kinetics			Second stage adsorption kinetic model			Internal diffusion model		
	K_{11}	K_{12}	K_{13}	K_{21}	K_{22}	K_{23}	K_{31}	K_{32}	K_{33}
15	0.4028	0.4125	0.4258	0.0005	0.0005	0.0007	6.6383	7.6814	10.0310
30	0.2222	0.2283	0.2516	0.0008	0.0008	0.0020	8.8530	10.0069	12.5866
45	0.1555	0.1650	0.1894	0.0009	0.0012	0.0040	8.3241	9.9073	11.5500
60	0.1212	0.1331	0.1531	0.0009	0.0017	0.0061	7.8002	9.4126	10.3254
75	0.1011	0.1142	0.1332	0.0011	0.0026	0.0110	7.4120	8.8496	9.4050
90	0.0869	0.1054	0.1171	0.0012	0.0057	0.01597	7.0013	8.3842	8.6383
105	0.0763	0.0934	0.0938	0.0013	0.0067	0.0068	6.6244	7.8130	7.9311
120	0.0685	0.1066	0.0836	0.0014	0.1189	0.0071	6.3152	7.4289	7.4390
135	0.0646	/	0.0738	0.0021	-0.0464	0.0060	6.1425	7.0239	7.0075
150	0.0644	0.0983	0.0838	0.0050	0.6666	0.0740	5.9923	6.6495	6.7402
165	0.0677	0.0809	0.0731	0.0208	0.1514	0.0403	5.7836	6.3378	6.4218
180	/	/	/	/	/	/	5.5685	6.0709	6.1596
$\bar{X}$	0.1301	0.1538	0.1526	0.0033	0.0827	0.0158	6.8721	7.9638	8.6863

As shown in Table 10, Kij(i, j=1, 2, 3), i=1, 2, 3, representing the three kinetic models of this study, namely primary, secondary and internal diffusion adsorption kinetic models; j=1, 2, 3, representing the sodium oleate concentrations of 1.10^{-4}, 2.10^{-4}, and 3.10^{-4} mol/dm^3, respectively. As can be seen from Table 10, the adsorption rates of the primary and secondary adsorption kinetics models are much smaller than that of the internal diffusion adsorption model; and the numerical trends of the adsorption kinetics and the internal expansion kinetics show a negative correlation under different models, and the K values of the secondary adsorption kinetics model are positively correlated with the adsorption rates, and thus can be considered as constants for the flotation adsorption of narrow grades of minerals. Through data comparison, it can be seen that the adsorption rates of the primary adsorption kinetics under different conditions are higher than those of the other adsorption kinetic models. This indicates that the adsorption rates of the primary adsorption kinetics are more helpful for the formation of adsorption of sodium oleate molecules on the surface of barite ore. And according to the kinetics of the internal diffusion model, the diffusion rate of sodium oleate in an aqueous solution is much higher than the adsorption rate of sodium oleate in an aqueous solution.

4. Conclusions

According to the flotation experiments before and after microwave radiation on barite, the flotation mechanism of $C_{18}H_{33}NaO_2$ on the mineral surface before and after microwave radiation was analyzed from the perspective of macroscopic and microscopic adsorption, and the conclusions are as follows：

1. Mineral flotation tests show that after the microwave treatment, the flotation recovery of barite, and DI water increases by 2.67%, and 3.35%, respectively, while that of the microwave action pulp and chemically added pulp decreases by 2.90% and 8.51%, respectively. This indicates that microwave action barite can improve flotation recovery (up to 95.27%). Before microwave radiation, the micellar dispersion system in alkaline conditions is more stable than in acidic conditions, with a stronger aggregation-resisting ability. After the microwave radiation, the stability of barite and deionized water in acidic and alkaline conditions is the same; as for mineral slurry, the micellar dispersion system in acidic conditions is more stable than in alkaline conditions, with a stronger aggregation-resisting ability and being less inclined to coagulation or coalescence.
2. When the amount of sodium oleate is 20, 40, 50, 60, and 80 mg/dm^3, respectively, the specific surface of barite increases by 5.38%, 3.63%, 4.41%, 5.41%, and 3.70%, respectively, after 30 sec of microwave action. Compared with that before microwave action, the specific area displays an

average increase of about 4.51%, indicating that it can promote more dense adsorption between the agent and the mineral and thus increase the flotation effect.

3. When the flotation time is within 180 sec, with the barite grade of 96.18% as the fitted maximum, the flotation rate calculated by the relevant equations of the primary kinetic model is consistent with the actual results, and the fitted results best reflect the real flotation results before and after the microwave action. Comparing the adsorption rates of adsorption kinetics under different models, it can be seen that the results of the primary adsorption kinetic model are larger, indicating that it is more helpful for the adsorption of sodium oleate molecules on the surface of barite. As is revealed by the results of the internal diffusion model kinetics, the diffusion rate of sodium oleate in an aqueous solution is much higher than the adsorption rate of sodium oleate in an aqueous solution.

Acknowledgments

This work was financially supported by the National Natural Science Foundation of China (No. 51964038), the Inner Mongolia Autonomous Region Key Technology Tackling Program Project (2020GG0148) and the Natural Science Foundation of Inner Mongolia Autonomous Region Fund on the surface project (2019MS05036).

References

BRIJLESH, K.N., KHUSHBOO, K., SADHAN, B, DEB, MANOJ, K.S., 2018. *Bhupendra Singh Tomar. Microwave-assisted dissolution of highly refractory dysprosium-titanate (Dy_2TiO_5) followed by chemical characterization for major and trace elements using ICP-MS, UV-visible spectroscopy and conventional methods.* Radiochimica Acta, 106(11).

CEN, P., BIAN, X., LIU, Z.N., GU, M.Y., WU, W.Y., LI, B.K., 2021. *Extraction of rare earths from bastnaesite concentrates: A critical review and perspective for the future.* Minerals Engineering, 171.

CHAU, T., BRUCKARD, W., KOH, P, NGUYEN, A., 2009. *A review of factors that affect contact angle and implications for flotation practice.* Advances in Colloid and Interface Science. 150(2), 106-115.

CRISTINA, R.A., CHRISTINE, V.P., ENCARNACIÓN, R.A., ANDREW, P., 2015. *The influence of pH on barite nucleation and growth.* Chemical Geology, 391.

DENG, J., LIU, C., YANG, S.Y., LI, H.Q., LIU, Y., 2019. *Flotation separation of barite from calcite using acidified water glass as the depressant.* Colloids and Surfaces A: Physicochemical and Engineering Aspects, 579.

DUAN, H., LIU, W.G., WANG, X.Y,. GU, X.W., SUN, W.H., PENG, X., Y., YUE, H., 2021. *Investigation on flotation separation of bastnaesite from calcite and barite with a novel surfactant: Octylamino-bis-(butanohydroxamic acid).* Separation and Purification Technology, 117792, 256.

FAN, X., KELLY, R.K., ROWSON, N., 2000. *Effect of microwave radiation on ilmenite flotation*. Canadian Metallurgical Quarterly. 39(3):247-254

GURPINAR, G., SONMEZ, E., BOZKURT, V., 2004. *Effect of ultrasonic treatment on flotation of calcite, barite and quartz.* Mineral Processing and Extractive Metallurgy, 113(2).

HARUO, S., YOSHIO, T., 2014. *The crystal structure of barite, β-$BaS0_4$, at high temperatures.* Zeitschrift für Kristallographie - Crystalline Materials, 191, 1-4.

JIANG, H.Y., ZHANG, F.F., CHEN, Z.J., ZHANG, H., QI, Y.C., 2022. *Effect of acidified sodium silicate on flotation separation behavior of barite and dolomite*. Comprehensive Utilization of Mineral Resources, 2:121-126.

KASIA, P., SHRUTI, S., KASIA, P., SHRUTI, S., 2016. *Price analysis: Graphite and barite. Industrial Minerals.*

LIU, C., WANG, Q.Q., YANG, S.Y., 2021. *Effects of barite size on the fluorite flotation using the reagent scheme of GS/ NaOl.* Colloids and Surfaces A: Physicochemical and Engineering Aspects, 626.

LU, Y., LIU, W.P., WANG, X.M., CHENG, H.G., CHENG, F.Q., JAN, M., 2020. *Lauryl phosphate flotation chemistry in barite flotation.* Minerals, 10(3).

MICHELE, E.M., 2020. *BARITE.* Mining Engineering, 72(7).

NANTAWAT, D., LEK, S., 2016. *Manoon Masniyom. Influence of air flow rate and immersion depth of designed flotation cell on barite beneficiation.* Materials Science Forum, 4310, 867-867.

NURIA, S.P., MELANIE, K., SABINO, V.V., GUNTRAM, J., 2015. *On the effect of carbonate on barite growth at elevated temperatures.* American Mineralogist, 98(7).

OBAIDI, S.A, AKYILDIRIM, H., GUNOGLU, K., AKKURT, I., 2020. *Neutron shielding calculation for barite-boron-water.* Acta Physica Polonica A, 137(4).

OGWUEGBU, M., ACHUSIM, U., ONYEDIKA, A.C., AYUK, A., 2011. *Flotation recovery of barite from ore using palm bunch based collector.* International Journal of Chemical Sciences. 9(3).

OZKAN, S.G., BAKTARHAN, B., GUNGOREN, C., DEMIR, I., 2020. *Effect of conventional and microwave thermal treatments on floatability of low- and high-rank lignites*. Energy Sources, Part A: Recovery, Utilization, and Environmental Effects 42, 2357-2369.

SADIK, A.Y., 2017. *Effects of barite sand addition on glass fiber reinforced concrete mechanical behavior*. International Journal Of Engineering & Applied Sciences, 9(4).

SATHTHASIVAM, J., LOGANATHAN, K., SARP, S., 2016. *An overview of oil-water separation using gas flotation systems.* Chemosphere.114. 671-680.

XIONG, W.L., DENG, J., ZHAO, K.L., WANG, W.Q., WANG, Y.H., WEI, D.Z., 2020. *Bastnaesite, barite, and calcite flotation behaviors with salicylhydroxamic acid as the collector.* Minerals, 10(3), 282-282.

WANG, Y., 2019. *Study on the flotation behavior of calcium- and silica-bearing minerals in barite and barite ore*. Guizhou University, China.

WANG, R.L., SUN, W.J., HAN, H.S., SUN, W., LU, Q.Q., WEI, Z., 2021. *Fluorite particles as a novel barite depressant in terms of surface transformation*. Minerals Engineering, 106877,166.

WU, J.X., LI, J., LIN, J.W., Y, S.W., LI, M., SU, W.R., 2021. *Analysis of the influence mechanism of microwave on barite flotation by infrared fitting spectroscop]*. Spectroscopy and Spectral Analysis, 41(10):3083-3091.

WU, J.X., LI, J., LIN, J.W., YI, S.W., LI, M., SU, W.R., 2021. *Influence mechanism of microwave on barite flotation based on infrared fitting spectrum analysis.* Spectroscopy and Spectral Analysis.41(10), 3083-3091.

YU, X., 2015. *Study on the effect of pretreatment on the flotation behavior of wolfram and calcium-bearing veinstone minerals.* Jiangxi University of Technology, China.

ZHAO, Y., LIU, S.Q., LI, X.J., LI, T.T., HOU, K., 2014. *Recovery of low grade barite ore by flotation in the southwest area of China.* Applied Mechanics and Materials, 3082, 543-547.

ZHOU, L., TERRENCE, M., MO, B., WANG, L., ZHANG, S., WANG, C.Y., 2020. *Raman study of barite and celestine at various temperatures*. Minerals,10(3).